Intermolecular Conformational Coupling and Free Energy Exchange Enhance the Catalytic Efficiency of Cardiac Muscle SERCA2a following the Relief of Phospholamban Inhibition†

James E. Mahaney,‡ R. Wayne Albers,§ Jason R. Waggoner,|| Howard C. Kutchai,⊥ and Jeffrey P. Froehlich*,@

Biomedical Science Division, Edward Via Virginia College of Osteopathic Medicine, Blacksburg, Virginia 24060, National Institute of Neurological Disease and Stroke, National Institutes of Health, Bethesda, Maryland 20892, Department of Pharmacology and Cell Biophysics, University of Cincinnati College of Medicine, Cincinnati, Ohio 45267, Department of Molecular Physiology and Biophysics, University of Virginia, Charlottesville, Virginia 22908, and Department of Biochemistry and Molecular Biology, University of Maryland School of Medicine, 108 North Greene Street, Baltimore, Maryland 21201-1503

Received September 15, 2004; Revised Manuscript Received March 24, 2005

ABSTRACT: Activation of cardiac muscle sarcoplasmic reticulum Ca^{2+}-ATPase (SERCA2a) by β_1-agonists involves cAMP- and PKA-dependent phosphorylation of phospholamban (PLB), which relieves the inhibitory effects of PLB on SERCA2a. To investigate the mechanism of SERCA2a activation, we compared the kinetic properties of SERCA2a expressed with (+) and without (−) PLB in High Five insect cell microsomes to those of SERCA1 and SERCA2a in native skeletal and cardiac muscle SR. Both native SERCA1 and expressed SERCA2a without PLB exhibited high-affinity (10−50 μM) activation of pre-steady-state catalytic site dephosphorylation by ATP, steady-state accumulation of the ADP-sensitive phosphoenzyme (E1P), and a rapid phase of EGTA-induced phosphoenzyme (E2P) hydrolysis. In contrast, SERCA2a in native cardiac SR vesicles and expressed SERCA2a with PLB lacked the high-affinity activation by ATP and the rapid phase of E2P hydrolysis, and exhibited low steady-state levels of E1P. The results indicate that the kinetic differences in Ca^{2+} transport between skeletal and cardiac SR are due to the presence of phospholamban in cardiac SR, and not due to isoform-dependent differences between SERCA1 and SERCA2a. Therefore, the results are discussed in terms of a model in which PLB interferes with SERCA2a oligomeric interactions, which are important for the mechanism of Ca^{2+} transport in skeletal muscle SERCA1 [Mahaney, J. E., Thomas, D. D., and Froehlich, J. P. (2004) *Biochemistry 43*, 4400−4416]. We propose that intermolecular coupling of SERCA2a molecules during catalytic cycling is obligatory for the changes in Ca^{2+} transport activity that accompany the relief of PLB inhibition of the cardiac SR Ca^{2+}-ATPase.

Activation of cardiac muscle sarcoplasmic reticulum (SR)[1] Ca^{2+}-ATPase (SERCA2a) by β_1-adrenergic agonists, which leads to enhanced coupled Ca^{2+} transport and cardiac sarcoplasmic reticulum (CSR) Ca^{2+} stores, involves PKA-dependent phosphorylation of an intrinsic low-molecular weight CSR protein, phospholamban (PLB) (*1*). Phosphorylation of PLB increases the apparent Ca^{2+} affinity (*2*) and V_{max} (*3*) of SERCA2a, reflecting the loss of regulatory (inhibitory) control by PLB. These effects on SERCA2a are associated with increased rates of phosphoenzyme (EP) formation (*4*, *5*) and decomposition (*3*, *4*), requiring a sustained input of free energy from ATP hydrolysis during catalytic cycling. The relief of SERCA2a inhibition by PLB also leads to a reduced Ca^{2+} efflux activity during ATP-dependent Ca^{2+} sequestration by CSR (*6*, *7*), suggesting that the energy barrier to pump reversal is raised during activation, leading to increased Ca^{2+} transport efficiency. The mechanism responsible for the increased catalytic efficiency of ATP energy utilization and the reduced Ca^{2+} efflux activity in SERCA2a following stimulation by β_1-agonists has not been elucidated.

Saturation transfer EPR (ST-EPR) measurements of spin-labeled SERCA2a in native CSR show that phosphorylation of PLB by cAMP-dependent PKA enhances interaction between Ca^{2+}-ATPase monomers (*8*). This is consistent with the hypothesis that the PLB-regulated CSR Ca^{2+} pump is

† This work was supported in part by a grant to J.E.M. from the American Heart Association, National (EIG 0040094N).

* To whom correspondence should be addressed: Department of Biochemistry and Molecular Biology, University of Maryland School of Medicine, 108 N. Greene St., Baltimore, MD 21201-1503. Phone: (410) 706-7469. Fax: (410) 706-8297. E-mail: froehlichj@grc.nia.nih.gov.

‡ Edward Via Virginia College of Osteopathic Medicine.

§ National Institutes of Health.

|| University of Cincinnati College of Medicine.

⊥ University of Virginia.

@ University of Maryland School of Medicine.

[1] Abbreviations: SR, sarcoplasmic reticulum; SERCA, sarco(endo)-plasmic reticulum Ca^{2+}-transporting adenosine triphosphatase; PLB, phospholamban; CSR, cardiac sarcoplasmic reticulum; SSR, skeletal muscle sarcoplasmic reticulum; HF, High Five; PKA, protein kinase A; 2D12, anti-phospholamban monoclonal antibody; cAMP, cyclic adenosine monophosphate; EGTA, ethylenebis(oxyethylenenitrilo)-tetraacetic acid; PCA, perchloric acid; TCA, trichloroacetic acid; MOPS, 3-(*N*-morpholino)propanesulfonic acid; $C_{12}E_8$, polyoxyethylene 8-lauryl ether; EP, phosphoenzyme; P_i, inorganic phosphate; ST-EPR, saturation transfer electron paramagnetic resonance spectroscopy.

10.1021/bi048011i CCC: $30.25
Published on Web 05/05/2005

functionally monomeric, whereas SERCA2a uncoupled from PLB is functionally oligomeric. Unlike the skeletal muscle Ca^{2+}-ATPase isoform (SERCA1) (*9*), native CSR SERCA2a does not show allosteric activation of pre-steady-state dephosphorylation by ATP in the micromolar concentration range (*10*). High-affinity activation by ATP of the intermediate reactions downstream from phosphorylation is characteristic of the kinetic behavior of SERCA1 (*9*, *11*), which has a single nucleotide binding site in the cytoplasmic N domain as demonstrated by X-ray diffraction measurements (*12*). In addition to the allosteric effects of ATP, the stable accumulation of the ADP-sensitive phosphoenzyme (E1P) after the first turnover (*13*, *14*) and its disappearance upon treatment with a monomer-forming detergent ($C_{12}E_8$) (*11*, *15*) have been interpreted as evidence for oligomeric behavior in SERCA1 (*16*, *17*). Sensitivity to $C_{12}E_8$ has also been demonstrated in the rapid phase of E2P hydrolysis in SERCA1 observed after chasing with EGTA (*18*). The absence of this phase in native SERCA2a (*10*) is consistent with the lower turnover and V_{max} that distinguish the cardiac muscle isoform from SERCA1. PKA-dependent phosphorylation of PLB in native CSR activates phosphoenzyme decomposition (*3*, *4*) like the naturally occurring fast phase of E2P hydrolysis in fast skeletal muscle SR. The accelerated phosphoenzyme turnover and the ST-EPR spectral changes resulting from cyclic AMP and PKA-dependent phosphorylation of PLB (*8*) both suggest that activation of the cardiac muscle SR Ca^{2+} pump by the β_1-agonist-mediated signaling cascade involves SERCA2a oligomer formation.

In this investigation, we evaluated the changes in the kinetic behavior of the cardiac SR Ca^{2+} pump associated with the relief of SERCA2a regulation by PLB. SERCA2a was expressed with (+) or without (−) PLB in High Five (HF) insect cells using recombinant baculovirus transfection (*19*) as a means of characterizing PLB-dependent Ca^{2+} pump regulation. Endoplasmic reticulum microsomes isolated from transfected HF cells contained SERCA2a and PLB expressed at levels comparable to those found in the native CSR preparations with functional properties similar to those of SERCA2a and PLB in native cardiac SR membranes (*10*, *19*). Quenched-flow mixing was used to evaluate the kinetic properties of expressed SERCA2a in these microsomal membrane fractions for comparison with those of SERCA1 and SERCA2a in native membrane preparations. Specifically, we investigated the kinetics of transient phosphoenzyme formation and decay at different ATP concentrations and assessed E1P formation and spontaneous E2P hydrolysis in the steady state using ADP and EGTA to dephosphorylate the phosphoenzyme. Measurements of the steady-state $^{45}Ca^{2+}$ uptake and Ca^{2+}-ATPase activities in SERCA2a with PLB and SERCA2a without PLB were carried out (*19*) to determine how changes in the overall pump activity correlate with the kinetic behavior of the Ca^{2+}-ATPase intermediate reactions in the transient state. The results of these experiments show that the kinetic properties of SERCA2a coexpressed with PLB closely resemble those found in native cardiac muscle SR, whereas SERCA2a without PLB behaves like native skeletal SERCA1 with respect to allosteric activation by ATP, steady-state E1P accumulation, and E2P hydrolysis. These similarities suggest that the removal of PLB and its inhibitory control of SERCA2a transform the cardiac muscle Ca^{2+}-ATPase into an enzyme with kinetic properties closely resembling those of the skeletal muscle isoform, SERCA1. We have incorporated these features into a molecular model for β_1-agonist activation of the CSR Ca^{2+} pump in which Ca^{2+}-ATPase oligomer formation (*8*, *20*−*26*) and interprotomeric free energy transfer (*14*, *36*) are associated with the relief of inhibition of SERCA2a by PLB.

MATERIALS AND METHODS

Enzyme Preparation. Native skeletal SR (SSR) membranes containing SERCA1 were prepared from the fast-twitch hind leg and back muscles of New Zealand white rabbits as previously described (*13*). The average yield of SSR protein was ∼1 mg/g of tissue (wet weight), and the maximum phosphorylation capacity was 3−4 nmol/mg of protein, representing approximately half of the total Ca^{2+}-ATPase site density (*9*, *17*). Native cardiac SR (CSR) membranes containing the SERCA2a Ca^{2+}-ATPase isoform and PLB (in a predominantly unphosphorylated state) were prepared from canine left ventricular muscle using a previously described method (*10*, *27*) with slight modification. Finely minced left ventricular tissue from fresh canine myocardium was added to ice-cold 10 mM $NaHCO_3$ (pH unadjusted) at a weight-to-volume ratio of 1:5 and homogenized in a Warring blender (three bursts for 30 s separated by 30 s intervals). The myofilaments and mitochondria were removed by two centrifugations at 11500*g* for 20 min each and the CSR membrane vesicles recovered from the second supernatant by centrifugation at 143000*g* for 45 min. The protein pellet was suspended in 0.6 M KCl and 10 mM MOPS (pH 7.0) with stirring for 20 min to remove actomyosin and was recovered by a final centrifugation at 143000*g*. The average yield and a maximum phosphorylation capacity of the CSR membrane vesicles were approximately one-third (∼0.3 mg/g of tissue) and one-tenth (0.3−0.4 nmol/mg of protein) of their skeletal muscle counterparts, respectively. Native CSR and SSR membranes, suspended in 0.1 M KCl and 10 mM MOPS (pH 7.0) at a final protein concentration of 5−10 mg/mL, were frozen and stored in liquid nitrogen. A separate aliquot of the vesicles used in the Ca^{2+} uptake measurements was suspended in 0.25 M sucrose and 20 mM MOPS (pH 7) to prevent vesicle rupture during freezing and storage in liquid nitrogen.

Canine SERCA2a was expressed in the absence or presence of canine PLB in High Five cells using the baculovirus expression system as described elsewhere (*19*). Microsomes (predominantly endoplasmic reticulum vesicles) containing the expressed proteins were harvested 48 h after baculovirus infection, suspended in 250 mM sucrose and 10 mM histidine (pH 7.4), and stored in small aliquots at −80 °C. The amount of SERCA2a and phospholamban in the microsomes was quantified by protein assay, gel electrophoresis, and immunoblotting techniques using methods described previously (*19*). Several different preparations of expressed SERCA2a without or with coexpressed PLB were used in these studies. For the experiments presented in Figure 1, the Ca^{2+}-ATPase content of the microsomes was very carefully matched at 16% of the total protein by weight; the relative proportion of Ca^{2+}-ATPase to PLB coexpressed in the microsomes was between 1 and 2 mol of PLB/mol of Ca^{2+}-ATPase. For the rapid mixing experiments presented in Figures 2−4, the Ca^{2+}-ATPase content of the microsomes

varied between 16 and 20% of the total protein by weight and the PLB-to-Ca^{2+}-ATPase ratio was 3:1. For all preparations, the Ca^{2+}-ATPase was under full regulatory control by PLB when the two proteins were coexpressed, as determined by assays of Ca^{2+}-dependent ATPase and Ca^{2+} uptake activity conducted in the presence and absence of an anti-PLB antibody, as described below (see also Figure 1).

Steady-State Ca^{2+} Uptake and Ca^{2+}-ATPase Assays. The ATP-dependent Ca^{2+} uptake activity in tightly sealed insect cell ER microsomes expressing SERCA2a alone and SERCA2a with PLB was measured at 37 °C using $^{45}Ca^{2+}$ and the Millipore filtration technique as previously described (*19*). The incubation medium contained 0.1 mg/mL microsomal protein, 50 mM MOPS (pH 7.0), 100 mM KCl, 3 mM $MgCl_2$, 10 mM sodium oxalate, 1 mM EGTA, and 0−1.0 mM $CaCl_2$ which gave the desired ionized Ca^{2+} concentration, as previously determined (*19*). The reaction was initiated by the addition of 5 mM MgATP and terminated at various times afterward (0−15 min) by manual filtration of an aliquot of the incubation medium. The filters were washed twice with 5 mL of ice-cold 150 mM NaCl, and the amount of $^{45}Ca^{2+}$ that accumulated inside was measured by liquid scintillation counting. Prior to measurement of the $^{45}Ca^{2+}$ uptake activity, SERCA2a samples were incubated for 20 min on ice with or without anti-PLB monoclonal antibody 2D12 at an antibody-to-protein weight ratio of 1:1 (*19*). Incubation of PLB with this antibody has been shown to relieve the inhibition of SERCA2a by PLB, thus mimicking the effect of phosphorylation by protein kinase A in the presence of cAMP (*19*, *28*). The Ca^{2+}-ATPase activity of the expressed SERCA2a samples in insect cell microsomes was measured in an incubation medium containing 0.1 mg/mL microsomal protein, 50 mM MOPS (pH 7.0), 100 mM KCl, 3 mM $MgCl_2$, 1 mM EGTA, and 0−1.0 mM $CaCl_2$ to give the desired ionized Ca^{2+} concentration (*19*). The reaction was initiated by the addition of 5 mM MgATP, and inorganic phosphate liberation was assessed at various times afterward (0−10 min) by using the malachite green ammonium molybdate reagent to monitor inorganic phosphate production as previously described (*19*, *28*). For the Ca^{2+}-ATPase activity measurements, the microsomes were pretreated with 20 μg of the Ca^{2+} ionophore A23187 per milligram of total protein prior to the addition of MgATP to prevent the formation of a Ca^{2+} transport gradient across the membrane (*19*). Preincubation with anti-PLB monoclonal antibody 2D12 prior to the Ca^{2+}-ATPase assay was essentially as described above. Calcium-dependent SERCA2a ATPase and Ca^{2+} uptake activity data were fit to the Hill equation using KFIT (*19*). The best fit, which produced values for the Hill coefficient (n), $K_{0.5}$, and V_{max} for the Ca^{2+}-ATPase and Ca^{2+} uptake activities, was chosen on the basis of the minimization of the sum-of-squares error (χ^2). Values given in the text represent the average of five independent repetitions, ± standard error of the mean.

Rapid Mixing Studies. One- and two-stage rapid mixing experiments were performed using a stepping motor-driven chemical quenched-flow apparatus that mixes equal volumes of reagents (*29*). Identical incubation conditions were used for investigating the kinetic behavior of the Ca^{2+}-ATPases present in native cardiac and skeletal muscle SR membrane vesicles and expressed in HF insect cell microsomes. ATP-dependent phosphorylation of the cardiac and skeletal Ca^{2+}-ATPase isoforms was assessed at 21 °C by mixing enzyme (0.5−0.75 mg/mL) suspended in a medium containing 100 mM KCl, 3 mM $MgCl_2$, 0.1 mM EGTA, 0.1 mM $CaCl_2$ (free $[Ca^{2+}] \approx 10$ μM), and 20 mM MOPS (pH 6.8) with an equal volume of a substrate solution containing 20 or 100 μM [γ-^{32}P]ATP. The reaction was terminated at the indicated times (0−300 ms) by the addition of 3% perchloric acid and 2 mM H_3PO_4 (final concentrations). [^{32}P]Phosphoenzyme was isolated from the acid-quenched reaction mixture by centrifugation for 10 min at 3000*g* and 4 °C and washed three times with a solution containing 5% trichloroacetic acid, 6% polyphosphoric acid, 4 mM H_3PO_4, and 5 mM unlabeled ATP. The pellet recovery after washing was greater than 95% as determined by a folin reagent protein assay. The protein pellets were dissolved overnight in 5 mL of 1 N NaOH, and the amount of [^{32}P]phosphoenzyme was determined by measuring the Cerenkov radiation in a scintillation counter (*17*).

To measure the kinetics of dephosphorylation by ADP and EGTA, the native and expressed SERCA isoforms were phosphorylated as described above for a constant time interval and then dephosphorylated for a variable time interval by mixing them with the appropriate chase solution. Steady-state formation of the ADP-sensitive phosphoenzyme was assessed by phosphorylating the enzyme with 10 μM [γ-^{32}P]ATP for 116 ms and chasing with a solution containing 15 mM ADP (5 mM after mixing), 100 mM KCl, 3 mM $MgCl_2$, 0.1 mM EGTA, 0.1 mM $CaCl_2$, and 20 mM MOPS (pH 6.8) at 21 °C. Dephosphorylation was allowed to proceed for a variable time interval (0−542 ms) after which the reaction was terminated by the addition of 3% perchloric acid and 2 mM H_3PO_4. The initial disappearance of phosphoenzyme, reflecting resynthesis of ATP from E1P and ADP (*11*, *13*), was used to estimate the fraction of ADP-sensitive E1P. The kinetics of E2P hydrolysis in the steady state was measured by chasing the phosphoenzyme formed at 10 μM [γ-^{32}P]ATP for 116 ms with a solution containing 15 mM EGTA (5 mM after mixing), 100 mM KCl, 3 mM $MgCl_2$, and 20 mM MOPS (pH 6.8) at 21 °C. Chelation of the ionized Ca^{2+} by EGTA prevents rephosphorylation of the enzyme, exposing spontaneous turnover of the ADP-insensitive phosphoenzyme, E2P (*10*). [^{32}P]Phosphoenzyme present in the ADP and EGTA chase experiments was separated from the acid-quenched reaction mixture by centrifugation, washed, and analyzed as described above.

Modeling of Kinetic Data. The rate constants for transient phosphoenzyme (EP) formation and overshoot decay were evaluated from the time course of phosphorylation at different ATP levels by fitting the quenched-flow data to the following equation using MLAB (Civilized Software):

$$[EP]_t = A_1 \exp(-k_p t) + A_2 \exp(-k_d t) + R \qquad (1)$$

where k_p and k_d are the rate coefficients for the rising and falling phases of phosphorylation, respectively, A_1 and A_2 are the corresponding amplitude coefficients, and R is the residual phosphoenzyme, corresponding to the steady-state level of phosphorylation. With increasing time, the first two terms on the right-hand side of the equation approach zero, leaving [EP] equal to R. This approach was used in lieu of the standard procedure of fitting the data to a reaction scheme

defined by a set of differential equations that are simultaneously integrated during the fitting operation. This was done to minimize the number of kinetic parameters needed to fit the curves and reduce their interdependence on one another. The fitted rate constants correspond to different intermediate steps in the reaction cycle depending on the experimental conditions. In Table 1, k_p at a less-than-saturating ATP concentration is the rate constant of the ATP binding reaction (E1 + ATP → E1·ATP), and for [ATP] > [E_{total}], k_p equals k_{ATP}[ATP], where k_{ATP} is the second-order rate constant for ATP binding. At a saturating ATP concentration, k_p equals k_{PHOS}, the rate constant for E1P formation (E1·ATP → E1P + ADP). The rate of decay of the phosphoenzyme overshoot is k_d, which is primarily dependent on E2P hydrolysis (E2P → E2 + P_i) but also depends on the E2 → E1 step, the final step in the reaction cycle. For a simple model in which ATP enters the reaction cycle at a single step (viz., ATP binding to E1), k_p is expected to vary with ATP concentration at less-than-saturating concentrations, whereas k_d is independent of ATP concentration because E2P hydrolysis obeys first-order kinetics. In the case of allosteric activation by ATP, where substrate enters the cycle at more than one step, k_d will vary if ATP enters the cycle downstream from phosphorylation and accelerates the breakdown of E2P (second-order kinetics). Variation in k_d can thus be used to distinguish ATP-dependent allosteric behavior from a simple model in which ATP binds only to E1 to form the Michaelis complex, E1·ATP.

The rate and amplitude coefficients for dephosphorylation induced by mixing the phosphorylated enzyme with ADP or EGTA were evaluated by fitting the quenched-flow data to a triexponential decay equation using MLAB:

$$[EP]_t = A_1 \exp(-k_1 t) + A_2 \exp(-k_2 t) + A_3 \exp(-k_3 t) \quad (2)$$

where k_i terms ($i = 1-3$) are the rate constants for the different phases of EP decay and A_i terms ($i = 1-3$) are the corresponding amplitude coefficients. In the ADP chase experiments, A_1, A_2, and A_3 correspond to the levels of the ADP-sensitive phosphoenzyme, E1P, the ADP-insensitive phosphoenzyme, E2P, and the stable phosphoenzyme, ESP, respectively (*11*, *13*). E1P and E2P are consecutive intermediates in the main catalytic pathway, whereas ESP is relegated to a parallel pathway because of its extremely slow turnover rate (~1 s^{-1}). The decay patterns in the EGTA chase experiments arise from spontaneous E2P hydrolysis and show a variable pattern of behavior depending on the Ca^{2+}-ATPase isoform that is used. In the case of native skeletal SERCA1 and expressed cardiac SERCA2a, a triexponential fit was required to fit the initial lag in dephosphorylation preceding the rapid and slow decay phases. In contrast, both native cardiac SERCA2a and expressed cardiac SERCA2a with coexpressed PLB lacked the rapid decay phase and were adequately fit with two slowly decaying exponential functions. The choice of whether to use a biexponential fit versus a triexponenetial fit was determined by comparison of the residual error between the fitted curve and actual data. When similar residual errors were obtained with the biexponential and triexponential fits, the simpler equation was chosen.

Kinetic and Free Energy Changes Associated with Chemical Coupling. The theory of absolute reaction rates (*30*) was used to estimate the free energy change associated with an increase or decrease in the forward rate constant, k_f, induced by chemical coupling. $k_f = A \exp(-G^{\ddagger}/RT)$, where $G^{\ddagger}$ is the free energy difference between the ground state and the activated or transition state in kilocalories, A is a preexponential factor determining the rate at which a molecule in the transition state is transformed into product, and R (1.98 cal deg^{-1} mol^{-1}) and T (temperature, kelvin) have their usual meanings. If $G^{\ddagger}$ represents the energy barrier for the E1P → E2P conformational transition in the uncoupled, monomeric Ca^{2+}-ATPase (e.g., SERCA2a with PLB), then coupling this transition to a slow reaction in the oligomeric enzyme (e.g., SERCA2a without PLB) will raise the energy barrier by an amount G^U so that the total energy becomes $G^{\ddagger} + G^U$. By application of this load and raising the energy barrier for the conformational transition, the rate constant for the transition is reduced and E1P accumulates in the steady state. The reduced rate constant k_f* for the E1P → E2P transition in the presence of the load is equal to $A \exp[-(G^{\ddagger} + G^U)/RT] = k_f \exp(-G^U/RT)$, where $k_f > k_f$*. A similar expression can be derived for k_f in the case where the transition-state energy barrier is lowered by an amount $-G^U$ by coupling to an energy-yielding reaction; $k_f^* = A \exp[-(G^{\ddagger} - G^U)/RT] = k_f \exp(G^U/RT)$, where $k_f^* > k_f$. In this case, coupling increases the rate constant by an amount equal to $\exp(G^U/RT)$. If these equations are rearranged, the magnitude of the increase (or decrease) in the barrier energy produced by coupling is given by the equation $G^U = |\pm RT \ln k_f/k_f^*|$. Thus, the ratio of the rate constants before and after coupling is the variable that defines the magnitude of the free energy difference associated with the change in the kinetic behavior of a specific reaction. This model of energy coupling is analogous to that of Läuger and Stark (*31*), who calculated the change in the translocation rate for a charged carrier complex in the presence of similar (accelerating) and opposing (decelerating) membrane voltages.

RESULTS

Regulation of SERCA2a $^{45}Ca^{2+}$ Uptake and Ca^{2+}-ATPase Activities by Phospholamban. High Five insect cell microsomes containing expressed SERCA2a without PLB or SERCA2a with PLB were produced and characterized as described previously (*19*). The SERCA2a coexpressed with PLB was under the full regulatory control of PLB, which increased the $K_{0.5}$ for the high-affinity Ca^{2+} transport sites relative to SERCA2a without PLB and for PLB uncoupled from SERCA2a following treatment with anti-PLB monoclonal antibody 2D12 (*19*, *28*). This is demonstrated in Figure 1, which shows the Ca^{2+} concentration dependencies of Ca^{2+} uptake (panel A) and of ATPase activity (panel B) of the expressed Ca^{2+}-ATPase proteins.

Figure 1A shows the Ca^{2+} concentration-dependent Ca^{2+} uptake activity for the expressed samples. SERCA2a without phospholamban [Figure 1 (○)] had a higher apparent Ca^{2+} affinity ($K_{0.5}$ = 125 ± 4 nM) than did SERCA2a in the presence of PLB ($K_{0.5}$ = 185 ± 5 nM). In addition, in microsomes containing SERCA2a expressed alone [Figure 1A (○)], the V_{max} for Ca^{2+} uptake [220 ± 10 nmol of Ca^{2+} min^{-1} (mg of protein)$^{-1}$] was 57% larger than the corresponding value [140 ± 8 nmol of Ca^{2+} min^{-1} (mg of protein)$^{-1}$] for microsomes containing SERCA2a with PLB [Figure 1A (□)]. The samples used in this experiment were carefully matched for SERCA2a content (~16 wt % total

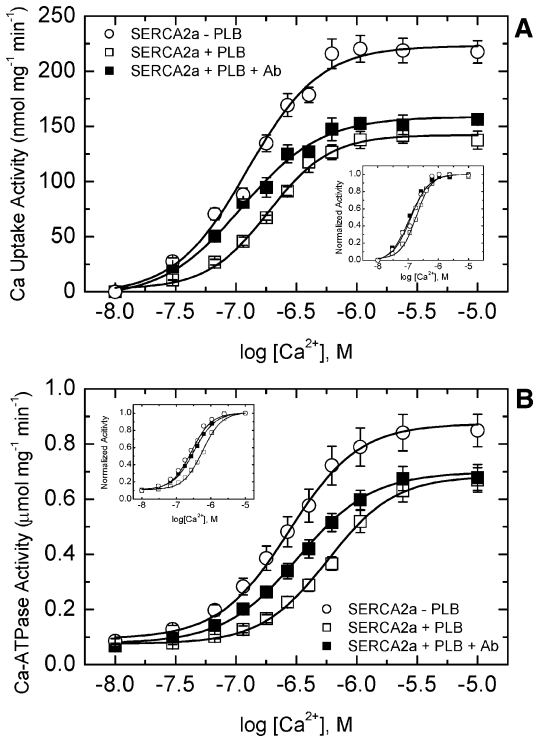

FIGURE 1: Effect of PLB and anti-PLB monoclonal antibody 2D12 on the steady-state Ca^{2+} uptake and Ca^{2+}-ATPase activities of expressed SERCA2a in High Five insect cell microsomes. (A) ATP-dependent oxalate-supported Ca^{2+} uptake activity of sealed microsomes (0.1 mg of total protein/mL) using the Millipore filtration technique and (B) ATP-dependent Ca^{2+}-ATPase activity of A23187-permeabilized microsomes (0.05 mg of total protein/mL) using the colorimetric technique. The same protein preparations were used in each experiment, and were carefully matched for SERCA2a protein content (16 wt % total protein). Microsomes containing SERCA2a alone (○) or SERCA2a and PLB (□ and ■) were assayed in a medium containing 50 mM MOPS (pH 7.0), 3 mM $MgCl_2$, 100 mM KCl, 1 mM EGTA, and 0−1.0 mM $CaCl_2$ to give the desired ionized Ca^{2+} concentration, as previously determined (*19*). For the Ca^{2+} uptake experiments, the medium also contained 10 mM sodium oxalate, whereas for the Ca^{2+}-ATPase experiments, the microsomes were pretreated with 20 μg of A23187/mg of protein in the incubation medium. The assays were conducted at 37 °C, and in each experiment, 5 mM MgATP was added to start the assay. SERCA2a samples were incubated for 20 min on ice without (empty symbols) or with (filled symbols) anti-PLB monoclonal antibody 2D12 at an antibody-to-protein weight ratio of 1:1 (*19*). Calcium-dependent SERCA2a ATPase and Ca^{2+} uptake activity data were fit to the Hill equation using KFIT (*19*) to generate values for the Hill coefficient (n), $K_{0.5}$, and V_{max}. The insets show each curve normalized to its maximum value, to more clearly demonstrate that uncoupling PLB from SERCA2a with an anti-PLB monoclonal antibody (■) produces a Ca^{2+} concentration dependence similar to that observed for SERCA2a in the absence of PLB. Symbols represent the average of five independent repetitions, and the error bars correspond to the standard error of the mean for each point.

protein; see Materials and Methods), indicating the observed differences in V_{max} were not due to different SERCA2a levels in the two samples. Rather, the higher V_{max} found in the absence of PLB suggests that the rate-limiting reactions in the transport cycle that contribute significantly to V_{max} are activated by the removal of the PLB-dependent inhibition of SERCA2a activity. Alternatively, the larger difference in V_{max} seen in the SERCA2a protein-matched samples may arise from a difference in the activities of the expressed proteins resulting in a larger fraction of more active SERCA2a when PLB is absent (*19*). Following treatment of the SERCA2a with PLB sample with anti-PLB monoclonal antibody 2D12 [Figure 1A (■)], $K_{0.5}$ decreased to 110 ± 10 nM, like that of the SERCA2a without PLB sample. In contrast, anti-PLB treatment of the SERCA2a with PLB sample produced only a modest (∼14%) increase in V_{max} [160 ± 2 nmol of Ca^{2+} min^{-1} (mg of protein)$^{-1}$] compared to that of the untreated SERCA2a- and PLB-containing microsomes [Figure 1A (□)], suggesting that phospholamban has a residual effect on SERCA2a activity following incubation with the antibody.

Figure 1B shows the Ca^{2+}-ATPase activity in microsomal membranes corresponding to the Ca^{2+} uptake data in Figure 1A. Prior to measurement of the Ca^{2+}-ATPase activity, the microsomes were preincubated with A23187 (20 μg/mg of protein) to increase their permeability to Ca^{2+} and prevent the formation of the transport gradient. The Ca^{2+} concentration dependence of these curves had an appearance similar to that of the curves in Figure 1A; in the absence of PLB, the SERCA2a activity curve (○) was shifted to the left ($K_{0.5}$ = 290 ± 40 nM) relative to that of SERCA2a with PLB (□) ($K_{0.5}$ = 590 ± 50 nM), and there was a larger V_{max} (0.85 ± 0.06 μmol of ATP mg^{-1} min^{-1}) compared to that of the SERCA2a with PLB sample (0.67 ± 0.04 μmol of ATP mg^{-1} min^{-1}), though the increase in V_{max} was smaller (27%) than that observed in the uptake measurements (57%). Pretreatment of the SERCA2a with PLB sample with the anti-PLB antibody [Figure 1B (■)] increased the apparent Ca^{2+} affinity ($K_{0.5}$ = 340 ± 40 nM) of the transport sites, but did not increase V_{max} (0.68 ± 0.05 μmol of ATP mg^{-1} min^{-1}) compared to that of the untreated SERCA2a with PLB sample [Figure 1B (□)].

Phosphorylation of Native and Expressed Ca^{2+}-ATPase Isoforms by ATP. The Ca^{2+}-ATPase in native skeletal SR membranes (SERCA1) exhibits ATP-dependent activation of pre-steady-state dephosphorylation at micromolar ATP concentrations (*9*, *11*). This is demonstrated in Figure 2A, which shows the time course of phosphorylation produced by mixing native skeletal SR membranes with 10 and 50 μM ATP in a quenched-flow apparatus. These experiments were carried out at 21 °C in a buffer containing 100 mM KCl, 3 mM $MgCl_2$, 20 mM MOPS (pH 6.8), and $CaCl_2$ and EGTA (0.1 mM each), yielding a free Ca^{2+} concentration of ∼10 μM (*19*), henceforth denoted as the standard buffer. The rate of phosphoenzyme formation increased rapidly to a maximum followed by a transient decay to the steady state. Increasing the ATP concentration from 10 to 50 μM increased the apparent rate constant for EP formation (k_p) 3-fold and doubled the rate of decay of the overshoot (k_d) following maximum accumulation (Table 1). Because the overshoot decay results from rapid breakdown of the ADP-insensitive phosphoenzyme (E2P) to inorganic phosphate (P_i) (*9*), the increase in k_d shows that E2P hydrolysis in SERCA1 is ATP-dependent, reflecting allosteric control by ATP (see Materials and Methods).

We investigated the effect of ATP concentration on the kinetics of phosphorylation in native cardiac muscle Ca^{2+}-ATPase (SERCA2a) under conditions identical to those used with native skeletal SR vesicles (Figure 2B). Typical of the behavior in cardiac SR (*3*, *4*, *10*), the level of phosphorylation was only ∼10% (∼0.3 nmol/mg of protein)

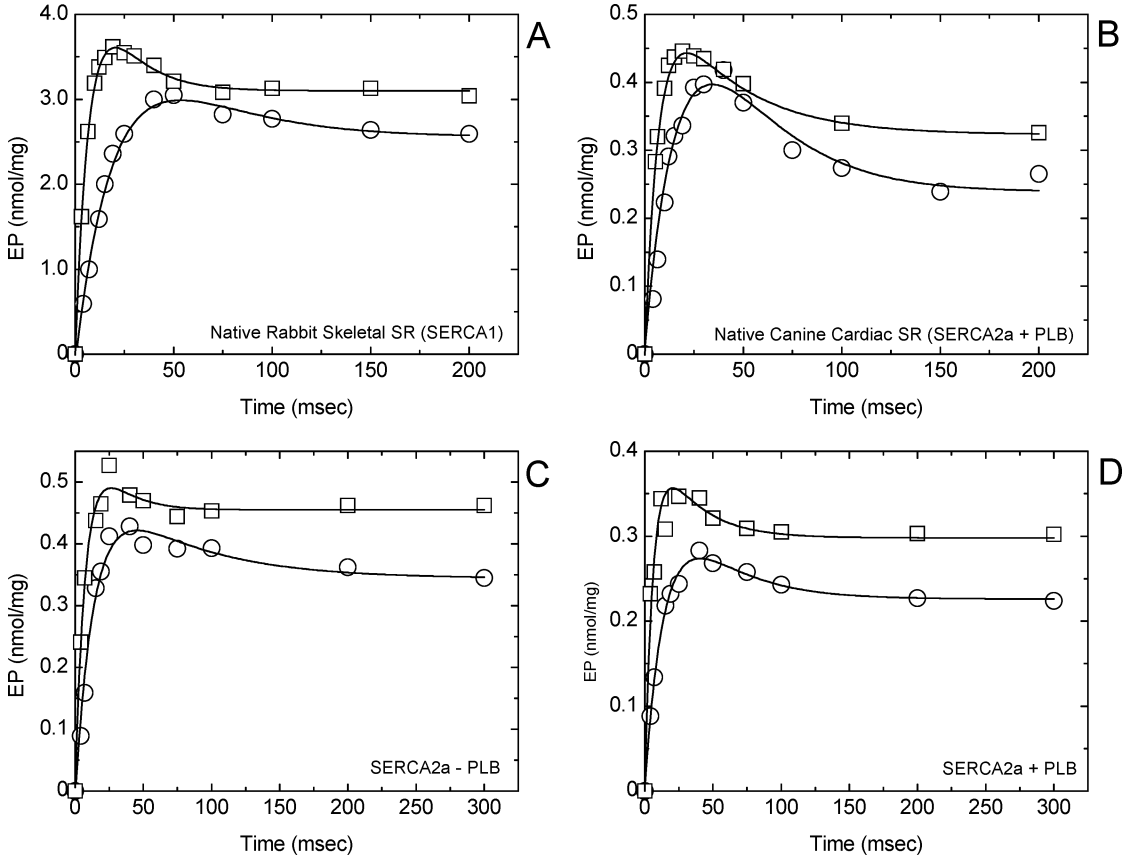

FIGURE 2: Effect of ATP concentration on pre-steady-state phosphoenzyme (EP) formation and decay in native and expressed cardiac and skeletal muscle SERCA isoforms: (A) native skeletal SR vesicles (containing SERCA1) (*13*), (B) native cardiac SR vesicles (containing expressed SERCA2a and PLB) (*10*), (C) High Five insect cell microsomes containing expressed SERCA2a alone, and (D) High Five insect cell microsomes containing expressed SERCA2a and PLB. Phosphoenzyme formation in each of these preparations was measured in a quenched-flow apparatus at 21 °C by mixing microsomes (0.5 mg/mL) suspended in a buffer containing 100 mM KCl, 3 mM $MgCl_2$, 0.1 mM $CaCl_2$, 0.1 mM EGTA (~10 μM ionized calcium), and 20 mM MOPS (pH 6.8) with an equal volume of the same solution containing either 20 μM [γ-^{32}P]ATP [10 μM final concentration (○)] or 100 μM [γ-^{32}P]ATP [50 μM final concentration (□)] (see Materials and Methods). The phosphorylation time courses were approximated with smooth curves by fitting the data to a sum of exponentials using MLAB (*48*) and eq. 1 (see Materials and Methods). Kinetic time courses from a single experiment are shown in this figure and Figures 3 and 4. Quantitatively similar time courses were obtained by independent experimental repeats in each case. The averaged kinetic parameters presented in the tables are from fits of the individual time courses.

of the maximal activity measured in skeletal muscle SR vesicles. The apparent rate constant for phosphoenzyme formation increased with increasing [ATP], concentration, rising 3-fold between 10 and 50 μM ATP. The rate constant controlling overshoot decay, however, did not increase with ATP concentration (Table 1), indicating that the kinetics of E2P hydrolysis in the cardiac muscle Ca^{2+}-ATPase in the presence of regulatory PLB is not allosterically regulated by ATP. The decay of the EP overshoot in native cardiac SR was more pronounced than in skeletal SR (cf. panels A and B of Figure 2), reflecting the presence of a slower E2 → E1 transition rate constant and stabilization of the cardiac muscle isoform in the dephosphorylated E2 state. In skeletal SR, the enzyme is more rapidly rephosphorylated after the first turnover, presumably because of a faster E2 → E1 transition, resulting in a higher steady-state level of phosphorylation.

To determine directly the effects of PLB on SERCA2a kinetics, we measured the ATP concentration-dependent phosphoenzyme formation of SERCA2a expressed in High Five insect cell microsomes at the same ATP concentrations (10 and 50 μM) used to investigate the native membrane preparations (Figures 2C and 2D). The level of expression of SERCA2a in the microsomes (15.8 ± 1.8 wt %) was similar to that found in native cardiac SR (35.6 ± 1.8 wt %) as demonstrated by the similarity in the steady-state levels of phosphorylation in these preparations (0.25−0.45 nmol of EP/mg of protein). As observed in native SERCA1, but unlike the behavior found in native cardiac SR, the ATP-dependent increase in the apparent rate constant for phosphorylation in expressed SERCA2a without PLB was accompanied by an increase in the rate of overshoot decay (Table 1), reflecting ATP-dependent activation of pre-steady-state dephosphorylation. Hence, removing PLB from the membrane changes the behavior of SERCA2a in the way it interacts with ATP, transforming the kinetics of dephosphorylation from simple first-order behavior in the presence of PLB to a second-order dependence on ATP concentration in the absence of PLB.

Identical phosphorylation experiments were carried out using High Five microsomes containing expressed SERCA2a with PLB (Figure 2D). These samples contained 20% SERCA2a by weight and produced steady-state EP levels similar to those of native cardiac SR membranes in proportion to SERCA2a protein content. The expressed SERCA2a with PLB sample displayed a rising phase of phosphorylation that was dependent on ATP concentration (Figure 2D) as observed in the other samples, but the overshoot decayed

Table 1: Kinetic Parameters of Pre-Steady State Phosphoenzyme (EP) Formation and Decay in Native and Expressed Cardiac and Skeletal SERCA Isozymes[a]

Preparation	[ATP] (μM)	k_p (s^{-1})	k_d (s^{-1})
Native skeletal SR (SERCA1)	10	42 ± 4	30 ± 3
	50	133 ± 13	59 ± 6
Native cardiac SR (SERCA2a + PLB)	10	45 ± 5	36 ± 4
	50	144 ± 14	27 ± 3
SERCA2a without PLB (insect cell microsomes)	10	71 ± 2	18 ± 3
	50	178 ± 52	42 ± 7
SERCA2a with PLB (insect cell microsomes)	10	57 ± 9	29 ± 5
	50	199 ± 35	31 ± 4

[a] Phosphorylation was measured as described in the legend of Figure 2, and the data were fitted to the equation $EP(t) = A_1 \exp(-k_p t) + A_2 \exp(-k_d t) + R$ using the curve fitting routines in MLAB (*48*). Rate constants k_p and k_d correspond to the rising and decaying phases of phosphorylation, respectively, and R is the steady-state EP level. The increase in k_d with an increase in ATP concentration reflects the allosteric activation of catalytic site dephosphorylation (E2P hydrolysis) by ATP in the pre-steady state. The kinetic constants in this and subsequent tables are average values obtained from two independent experiments, and the errors represent the difference between the average and the high and low value for each trial.

without a change in rate constant as the ATP concentration increased (Table 1), as in the native CSR sample. This is consistent with the results of Figure 2B which show the kinetics of E2P hydrolysis in the cardiac muscle Ca^{2+}-ATPase in the presence of PLB is not subject to allosteric regulation by micromolar [ATP].

Dephosphorylation of Native and Expressed Ca^{2+}-ATPase Isoforms by ADP. To determine the steady-state levels of E1P and E2P and their kinetic behavior, we performed a two-stage quenched-flow mixing experiment in which the time course of dephosphorylation of the Ca^{2+}-ATPase was investigated by chasing the phosphoenzyme formed from ATP with 5 mM ADP (*9*, *11*, *13*). Prior to mixing with ADP, the enzyme was incubated with 10 μM [γ-^{32}P]ATP in standard buffer for 116 ms to achieve a steady-state level of phosphorylation (see Figure 2A). For native SERCA1, 30 ± 6% of the phosphoenzyme disappeared rapidly in response to the ADP chase and was followed by a slower, time-resolved decay representing 70 ± 5% of the acid-stable EP pool (Figure 3A, top curve; Table 2). We have shown previously (*9*, *11*, *13*) that phosphoprotein disappearing during the fast phase is E1P (i.e., it reacts with ADP to form ATP) and that disappearing during the slow decay results from the breakdown of E2P to E2 and P_i. After 250 ms, a very slowly decaying species was observed, representing a third component of the decay pattern. Turnover of this species was too slow for it to be kinetically competent, justifying its subtraction from the total phosphoenzyme pool in the kinetic analysis (*13*).

Chasing the phosphoenzyme in native cardiac SR with 5 mM ADP produced a pattern of dephosphorylation qualitatively similar to that found in native SERCA1 (Figure 3A, bottom curve). Normalization of these ADP dephosphorylation data (inset of Figure 3A) revealed that the rapidly decaying E1P species represents a smaller fraction of the total acid-stable phosphoenzyme in native cardiac SR (18 ± 2%) than in native skeletal SR (30 ± 6%). When the ADP chase experiment was repeated using insect cell microsomes containing SERCA2a and PLB (Figure 3B, bottom curve), the decay pattern resembled that of native CSR in showing a smaller fraction of E1P (10%) and a slower E2P turnover rate (10 s^{-1}) than SERCA1 in native skeletal SR. In contrast, microsomes containing SERCA2a

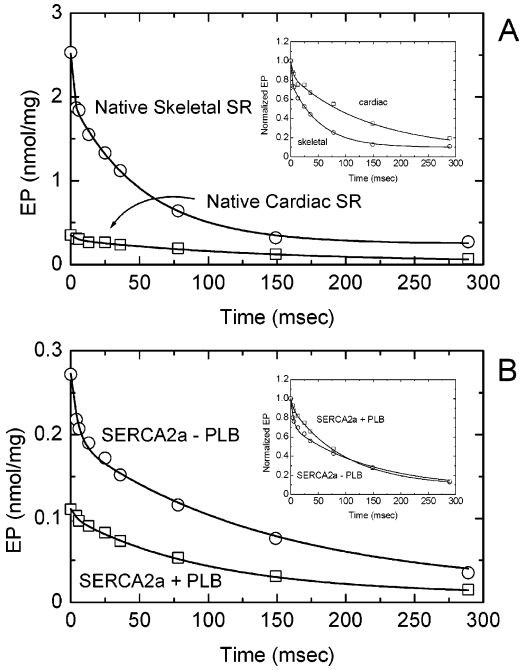

FIGURE 3: Dephosphorylation by ADP of the steady-state phosphoenzyme formed from ATP in native membranous and expressed SERCA isozymes. (A) Native skeletal muscle (○) and cardiac muscle (□) SR membranes or (B) High Five insect cell microsomes containing expressed SERCA2a alone (○) or SERCA2a with PLB (□) (0.5 mg/mL) were phosphorylated with 10 μM ATP as described in the legend of Figure 2. After 116 ms ($t = 0$ in the figure), a chase solution containing 5 mM ADP (1.66 mM final concentration) was added to the reaction mixture and dephosphorylation allowed to proceed for the indicated times before quenching with acid. ^{32}P-phosphoprotein was isolated from the reaction mixture and assayed as described in the legend of Figure 2. The difference in the time zero EP levels reflects differences in the level of Ca^{2+}-ATPase in the preparations used in these experiments. The insets show the data normalized to the phosphoenzyme level at time zero for each sample, to more clearly show the differences in levels of the phosphoenzyme intermediates. The dephosphorylation curves were fit to a multiexponential function using MLAB (*48*) as described in Materials and Methods.

Table 2: Kinetic Parameters of ADP-Induced Dephosphorylation in Native and Expressed Cardiac and Skeletal SERCA Isozymes[a]

Preparation	E1P (%)	k_f (s^{-1})	E2P (%)	k_s (s^{-1})
Native skeletal SR (SERCA1)	30 ± 6	>600	70 ± 5	20 ± 1
Native cardiac SR (SERCA2a + PLB)	18 ± 2	348 ± 112	82 ± 2	15 ± 9
SERCA2a without PLB (insect cell microsomes)	27 ± 4	220 ± 7	73 ± 4	9 ± 2
SERCA2a with PLB (insect cell microsomes)	10 ± 0	371 ± 130	90 ± 0	10 ± 0

[a] Dephosphorylation by ADP was assessed as described in the legend of Figure 3. The decay curve was fit (*48*) using the equation $EP(t) = [E1P] \exp(-k_f t) + [E2P] \exp(-k_s t) + [EPS] \exp(-k_{vs} t)$, where [E1P] and [E2P] are the steady-state levels of the ADP-sensitive and ADP-insensitive phosphoenzymes, respectively. The very slow decay (k_{vs}), representing turnover of a stable phosphoenzyme (EPS) parallel to the main catalytic pathway, was ignored in this analysis, i.e., %[E1P] + %[E2P] = 100% of the phosphoenzyme.

without PLB (Figure 3B, top curve) showed a steady-state fraction of E1P (27 ± 4%) similar to that found in native skeletal SR (30 ± 6%) but larger than that detected in native cardiac SR (18 ± 2%) and expressed SERCA2a and PLB (10%). Thus, the absence of PLB in native skeletal SR and in microsomes containing SERCA2a alone is associated with steady-state levels of E1P higher than those found in native cardiac SR and microsomal membranes containing PLB. Because the rate constants for E1P formation in the different preparations are very similar (Table 1), the dephosphorylation data suggest that the presence of PLB has a destabilizing effect on E1P, acting to increase its turnover rate. Conversely, the exclusion of PLB from these membranes inhibits E1P turnover, allowing the ADP-sensitive phosphoenzyme to accumulate in the steady state.

Dephosphorylation of Native and Expressed Ca^{2+}-ATPase Isoforms by EGTA. The standard approach for measuring the kinetics of E2P hydrolysis involves chelation of the free Ca^{2+} by EGTA, which exposes the spontaneous turnover of this intermediate by preventing rephosphorylation of the Ca^{2+}-ATPase during the subsequent cycle. As shown in Figure 4A, the time course of EGTA-induced E2P decomposition of the native cardiac muscle Ca^{2+}-ATPase obeyed slow monoexponential kinetics (8 s^{-1}) following a brief lag in which continued phosphorylation of the enzyme from E1(Ca_2)ATP occurs (*10*). In contrast, the skeletal muscle Ca^{2+}-ATPase showed a biphasic decay pattern with an initial phase that was 6−7 times faster (68 ± 16 s^{-1}) than the subsequent phase (7 s^{-1}). The latter, which accounts for 77% of [EP_{total}], dephosphorylates with kinetics similar to that of the monoexponential phase in the cardiac Ca^{2+}-ATPase (8 s^{-1}, Table 3). We conclude from these studies that spontaneous E2P hydrolysis, which is among the slowest of the reactions in the catalytic cycle, has a significantly higher initial activity in skeletal muscle SR than in native cardiac muscle SR. This kinetic characteristic and the higher density of Ca^{2+} pump sites in skeletal SR may contribute to the higher V_{max} of SERCA1 and faster rates of relaxation observed in skeletal muscle (*10*, *27*).

To determine how removal of phospholamban affects the kinetics of spontaneous dephosphorylation of SERCA2a, we phosphorylated insect cell microsomes containing SERCA2a alone with 10 μM ATP for 116 ms as described above and then chased the phosphoenzyme with 5 mM EGTA to prevent rephosphorylation. As shown in Figure 4B, phosphoenzyme decay after the chase shows a prominent lag phase (∼15−20 ms) followed by rapid and slow phases of dephosphorylation. The prolonged lag phase suggests that dissociation of Ca^{2+} from the high-affinity transport sites in the presence of the chelator may be slower in the microsomal membranes than in the native cardiac and skeletal SR preparations. Approximately 14 ± 1% of the phosphoenzyme disappeared in the fast phase with a rate constant of 63 ± 4 s^{-1}, while the remainder decayed at a slower rate of 3 s^{-1} (Table 3). This biphasic behavior resembles that found in native skeletal SERCA1, which turns over with similar kinetics, but has a larger rapid decay fraction (23 ± 7% of [EP_{total}]). An identical EGTA chase experiment performed with insect cell microsomes containing SERCA2a and PLB produced a monoexponential decay with a rate constant of 4 ± 1 s^{-1} following a brief lag (Table 3), similar to that observed for native canine cardiac SR. The use of a biexponential decay function did not improve the fit as determined by comparison of the sum-of-squares errors, indicating that the presence of PLB prevents the rapid phase of spontaneous dephosphorylation seen in SERCA1 and SERCA2a without PLB. The enzymatic similarities and differences recorded in these experiments parallel the behavior observed in the phosphorylation (Figure 2) and ADP chase experiments (Figure 3), namely, that SERCA2a without PLB exhibits catalytic behavior similar to that found in native

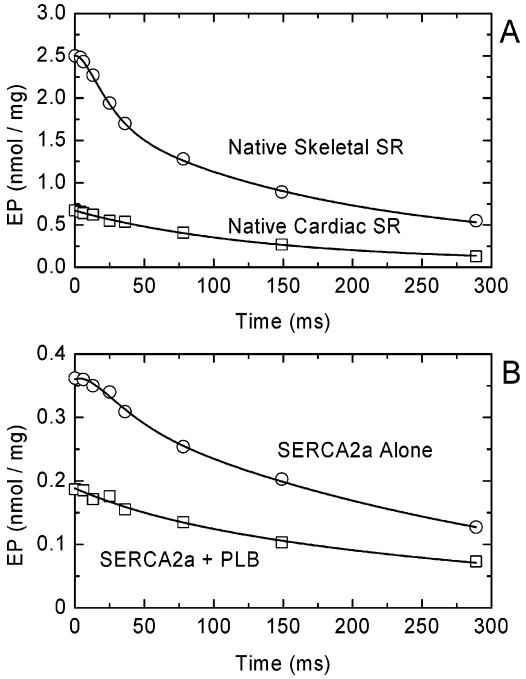

FIGURE 4: Spontaneous hydrolysis of E2P in the steady state measured by chasing with EGTA. (A) Native skeletal SR vesicles (○) and native cardiac SR vesicles (□) or (B) High Five cell microsomes containing expressed SERCA2a without PLB (○) or with PLB (□) were phosphorylated with 10 μM ATP as described in the legend of Figure 3. After 116 ms ($t = 0$ in the figure), a chase solution containing 15 mM EGTA (5 mM final concentration) was added to the reaction mixture and dephosphorylation was allowed to proceed for the indicated times before quenching with acid. ^{32}P-phosphoprotein was isolated from the reaction mixture and assayed as described in the legend of Figure 3. Inorganic phosphate (P_i) production after the chase (not shown) was stoichiometric with EP decay (*4*). The difference in the time zero EP levels reflects differences in the level of Ca^{2+}-ATPase in the preparations used in these experiments. The dephosphorylation curves were fit to multiexponential decay functions using MLAB (*48*).

Table 3: Kinetic Parameters of EGTA-Induced Dephosphorylation in Native and Expressed Cardiac and Skeletal SERCA Isozymes[a]

Preparation	fast E2P (%)	k_f (s^{-1})	slow E2P (%)	k_s (s^{-1})
Native skeletal SR (SERCA1)	23 ± 7	68 ± 16	77 ± 7	7 ± 0
Native cardiac SR (SERCA2a + PLB)			100 ± 0	8 ± 0
SERCA2a without PLB (insect cell microsomes)	14 ± 1	63 ± 4	86 ± 1	3 ± 1
SERCA2a with PLB (insect cell microsomes)			100 ± 0	4 ± 0

[a] Dephosphorylation by chasing with EGTA was assessed as described in the legend of Figure 4. Each decay curve was fit (*48*) using the equation $EP(t) = A_f \exp(-k_f t) + A_s \exp(-k_s t)$, where A_f and A_s and k_s and k_f are the amplitude and rate coefficients of the rapidly and slowly decaying phosphoenzymes, respectively. $\%A_f + \%A_s = 100\%$.

skeletal SERCA1 whereas SERCA2a coexpressed with PLB behaves like native cardiac SERCA2a.

DISCUSSION

In this study, we found that the cardiac (SERCA2a) and skeletal muscle (SERCA1) isoforms of the Ca^{2+}-ATPase in sarcoplasmic reticulum exhibit quantitative differences in kinetic behavior that relate to the influence of PLB on the Ca^{2+}-ATPase in CSR rather than isoform dependences in the two species. That is, removal of PLB and its regulatory influence on SERCA2a essentially transforms the cardiac muscle isoform into a species that resembles the skeletal muscle isoform, SERCA1, in its basic kinetic properties. We have previously reported that the kinetic properties of SERCA1 in native skeletal SR arise from oligomeric protein conformational interactions whereby the subunits operate in a staggered or out-of-phase mode of operation (*9*, *11*, *13*, *14*, *16*, *17*). Solubilization of skeletal SR vesicles with the nonionic detergent $C_{12}E_8$ produces SERCA1 monomers (*11*, *32*) and results in marked stimulation of E1P turnover and a decline in steady-state E1P levels (*11*, *15*, *33*) while abolishing the rapid phase of spontaneous E2P hydrolysis (*18*). Here we found that the exclusion of phospholamban from insect cell microsomes expressing SERCA2a, which mimics the activation of SERCA2a produced by cAMP and protein kinase A (*1*, *4*), increased the rate of phosphoenzyme overshoot decay measured at different ATP concentrations (Figure 2 and Table 1), and stimulated spontaneous E2P turnover in the steady state (Figure 4 and Table 3). Both of these effects result from activation of hydrolysis of the ADP-insensitive phosphoenzyme, E2P, and were associated with an increase in the steady-state level of E1P formation, reflecting stabilization of the ADP-sensitive intermediate (Figure 3 and Table 2). These kinetic properties are characteristic of the behavior observed for oligomeric SERCA1 in native skeletal muscle SR (*9*, *11*, *13*, *16*). In contrast, the kinetic properties of SERCA2a in native cardiac SR (*10*) or in microsomes containing coexpressed PLB resemble those of the detergent ($C_{12}E_8$)-solubilized (monomeric) SERCA1 (*11*), including reduced levels of E1P compared to those present in microsomes expressing SERCA2a alone and skeletal SR (Figure 3 and Table 2) and the absence of the rapid phase of spontaneous E2P hydrolysis (Figure 4 and Table 3). These properties are associated with lower overall Ca^{2+}-ATPase and Ca^{2+} uptake activities in the presence of PLB (Figure 1), since E2P turnover contributes to rate limitation of the overall catalytic and transport activities in SERCA2a. On the basis of these findings, we conclude that relief of PLB inhibition of the cardiac SR Ca^{2+}-ATPase leads to SERCA2a oligomer formation, providing a mechanism for the redistribution of the free energy in the system and enhancement of the overall catalytic efficiency.

Oligomeric interaction between individual SERCA2a molecules requires site-specific contact between the SERCA2a molecules, which we propose is prevented by the presence of unphosphorylated phospholamban, but facilitated when PLB is functionally uncoupled from SERCA2a following PLB phosphorylation. Recent studies by Squier and coworkers (*34*, *35*), using florescence resonance energy transfer studies to monitor the distance between PLB and SERCA2a, indicate that while PLB remains closely associated with the pump following cAMP/PKA-dependent phosphorylation, PLB structure becomes more compact, possibly exposing the N domain PLB binding site. Using saturation transfer electron paramagnetic (ST-EPR) spectroscopy to monitor the rotational diffusion of native cardiac SERCA2a, Negash et al. (*8*) reported a doubling of the rotational correlation time for spin-labeled SERCA2a following phosphorylation of phospholamban, consistent with a 2-fold increase in the molecular size of the Ca^{2+}-ATPase. A similar change was reported by Mahaney et al. (*36*), who used ST-EPR to measure SERCA2a rotational mobility in the absence and presence of PLB. Both studies attributed this behavior to a monomer−dimer transition in SERCA2a or to a conformational rearrangement favoring a more compact SERCA2a dimer. Either of these possibilities could lead to chemical coupling of the subunits and, consequently, a redistribution of the free energy of activation in the intermediate reactions of the pump cycle.

A hypothetical model accounting for the spectral and enzymatic changes in SERCA2a accompanying the relief of phospholamban inhibition is shown in Figure 5. In this model, the Ca^{2+}-stabilized E1 (*12*) and Ca^{2+}-free E2 (*37*) conformations form an asymmetric Ca^{2+}-ATPase dimer from monomeric precursor states, E1 and E2 (alternatively, the precursor may consist of two interacting monomers that form an uncoupled dimer; not shown). Dephosphorylated PLB or phosphorylated PLB is shown to be associated with the pump in both the E2 and E1 states, in agreement with fluorescence resonance energy transfer studies (*34*, *35*, *38*). On the basis of the crystal structure of SERCA1 in the E1 conformation (*12*), where physical contact is visible between the A and N domains of similarly oriented polypeptide chains, the A domain of one SERCA2a molecule is postulated to interact with the N domain of its neighbor, creating a bridge for intermolecular communication between the subunits. Phospholamban binding in this region of the P and N domains (*39*−*43*) would block SERCA2a oligomeric contact interactions, leading to a functionally monomeric enzyme during enzyme cycling. Structural changes in PLB following PLB phosphorylation (*34*, *35*) or removal of PLB from the membrane (this study) uncover the SERCA2a contact sites, allowing conformational coupling within a functional oligomeric enzyme during cycling. Because rotation of the A domain toward the N or P domain occurs during the E1 → E2 transition (*37*) and is essential for activation of dephosphorylation (*44*), delaying this rotation by means of an intermolecular A−N bridge during cycling will stabilize E1P, preventing its immediate conversion to E2P. Intermolecular bridging of these domains can also activate E2P hydrolysis by coupling it to an energy-yielding reaction (viz., E1P → E2P) on a neighboring subunit (*11*).

By constraining the subunits to an out-of-phase or staggered mode of operation (*11*, *13*, *17*, *18*, *45*), inherently fast reactions in the cycle (E1P → E2P) can be coupled to slow reactions (E2P → E2 + P_i), accelerating the latter through a mechanism involving free energy exchange (*14*, *31*). This, in turn, helps to relieve the rate limitation imposed by slow steps in the reaction cycle, thereby increasing the catalytic efficiency of the CSR Ca^{2+} pump. For the reaction pair E1P → E2P and E2P → E2 + P_i (Figure 5), the increase in the free energy of activation for the conformational transition on one subunit should be equivalent to the decrease in the free energy of activation for E2P hydrolysis on its neighbor if these reactions are tightly (efficiently) coupled (see

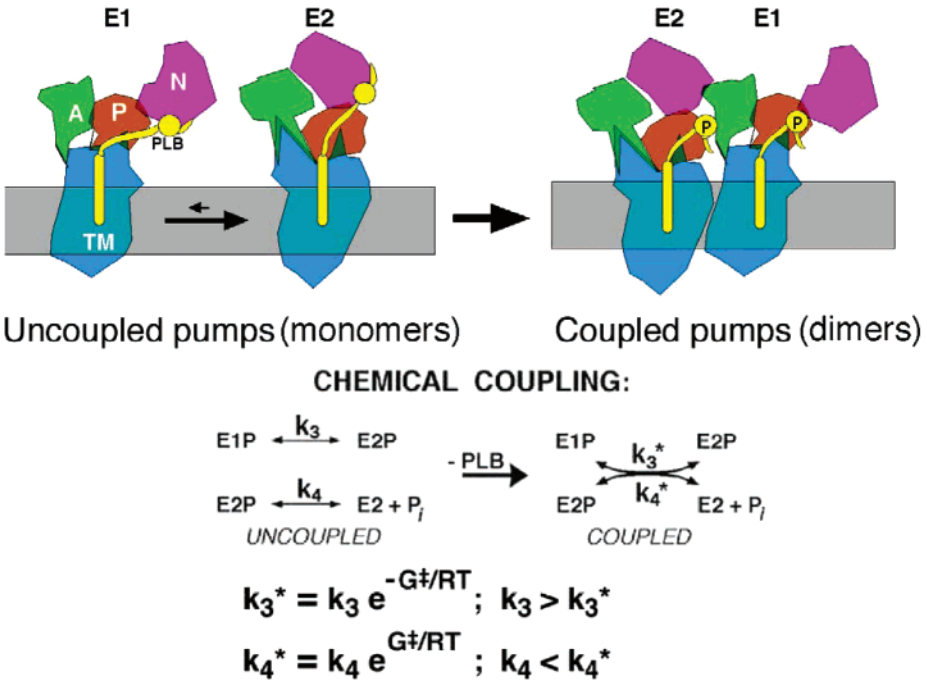

FIGURE 5: Oligomer model for β_1-adrenergic activation of SERCA2a. The crystal structures of SERCA1 in the Ca^{2+}-stabilized E1 (*12*) and thapsigargin-stabilized E2 conformations (*38*) were used to construct a three-dimensional topological model for SERCA2a intermolecular interactions regulated by PLB. PLB (yellow) is presumed to interact with SERCA2a at specific residues in the cytoplasmic nucleotide-binding domain (N, purple), the phosphorylation domain (red), and the transmembrane domain (TM, blue) (*2*, *31*−*33*). Interaction of SERCA2a with PLB stabilizes monomeric Ca^{2+}-ATPase on the left, which exists as an equilibrium of E1 and E2 states favoring the E2 conformation. Phosphorylation of PLB in response to β-agonist stimulation (represented by the P) exposes the N domain PLB binding site, which is then available to interact with the SERCA2a actuator domain (A, green) binding site on a neighboring SERCA2a molecule, forming the E2−E1 asymmetric dimer on the right. The individual subunits cycle according to the following model: E1 + ATP ←1→ E1·ATP ←2→ E1P ←3→ E2P ←4→ E2 + P_i ←5→ E1. Oligomerization of SERCA2a and staggering of the reactions in the subunits couples the fast conformational transition in step 3 to slow E2P hydrolysis in step 4. The equations for chemical coupling give the relationship between the rate constants for the reactions prior to (k_3 and k_4) and following oligomeric coupling (k_3* and k_4*) modified by the amount of free energy ($\pm G^{\ddagger}$) involved in the exchange (described in Materials and Methods). The reciprocal changes in rate constants k_3 and k_4 reflect the increase in the free energy of activation and consequent deceleration of one reaction (E1P → E2P transition) and the decrease in the free energy of activation by a second reaction (E2P → E2 + P_i), which is accelerated.

Materials and Methods). Indeed, removal of the inhibitory influence of phospholamban in the insect cell microsomes led to a 15-fold increase in the initial rate of spontaneous E2P hydrolysis [$k_4 = 4 \pm 1\ s^{-1} < k_4^* = 63 \pm 4\ s^{-1}$ (Table 3)] and increased the steady-state level of E1P by a factor of ~3 [10% vs 27 ± 4% (Table 2)], due to a reduced rate of conversion of E1P to E2P in the coupled oligomer versus the uncoupled enzyme ($k_3 > k_3^*$). Although the increase in E1P concentration implies a reduced rate of conversion to E2P, the quantitative comparison of these effects is complicated by the presence of the reverse rate constant, which is also reduced as a consequence of raising the transition-state energy barrier for this reaction. Thus, a decrease in the forward rate constant, which favors accumulation of E1P, is accompanied by a decrease in the reverse rate constant, tending to reduce the steady-state level of E1P. Additional studies are required to evaluate the reciprocal changes in rate constants attributed to conformational coupling of the subunits.

It is well established that PLB decreases the apparent Ca^{2+} affinity of the Ca^{2+}-ATPase, but the mechanistic basis of this effect has not been adequately explained. A commonly cited model is that reported by Cantilina et al. (*46*), who proposed that the shift in apparent Ca^{2+} affinity arises from PLB inhibition of the forward and reverse rate constants of the conformational transition that separates binding of the first and second Ca^{2+} ions (*47*). However, in subsequent studies, Mahaney et al. (28) showed that the rate of ATP-dependent SERCA2a phosphorylation under conditions where Ca^{2+} binding to SERCA2a was rate-limiting for phosphorylation did not differ in the presence or absence PLB, or in the presence of PLB pretreated with the anti-PLB antibody. In contrast, our model predicts that oligomerization of SERCA2a plays an essential role in the observed increase in the apparent affinity for Ca^{2+} ($\downarrow K_{0.5}$) following the relief of phospholamban inhibition (Figure 1). The decrease in the $K_{0.5}$ for Ca^{2+} is presumed to occur during enzymatic cycling because phospholamban has no effect on equilibrium Ca^{2+} binding in the quiescent Ca^{2+}-ATPase (*46*). If we assume that interaction of SERCA2a with unphosphorylated PLB stabilizes the E2 conformational state (*40*−*42*), then we have the situation on the left in Figure 5 where the equilibrium between the monomers favors E2. Formation of the asymmetric dimer, E1−E2, during cycling will equalize the populations of E1 and E2, which is tantamount to shifting the E1 ↔ E2 equilibrium toward E1. By increasing the fraction of enzyme in the high-affinity E1conformation, oligomerization of SERCA2a will enhance $E1Ca_2$ formation and shift the Ca^{2+} dependencies of the Ca^{2+} uptake and Ca^{2+}-ATPase activities to the left (Figure 1A,B). In this interpretation, the increase in the apparent Ca^{2+} affinity results from a change in the poise of the E1 ↔ E2

equilibrium driven by oligomerization of SERCA2a. Alternatively, intermolecular conformational coupling and free energy exchange during cycling may lower the $K_{0.5}$ by lowering the energy of activation for Ca^{2+} binding, resulting in an increase in the forward rate constant for Ca^{2+} binding to E1, analogous to the activation of E2P hydrolysis discussed above. This seems unlikely, however, given the finding that PLB does not affect equilibrium Ca^{2+} binding to the enzyme (*46*).

We (Figure 1) and others (*3*) have observed an increase in V_{max} for Ca^{2+} sequestration when the regulatory control of PLB is removed either by its exclusion from the membrane (this study), by anti-PLB antibody treatment, or by phosphorylation of PLB (*3*). In addition, there have been two reports of a reduction in Ca^{2+} efflux activity activated by phosphorylation of phospholamban (*6*, *7*). These changes in enzyme turnover and Ca^{2+} efflux activity indicate the ability of the cardiac pump to operate with an increased catalytic efficiency in the presence of a Ca^{2+} transport gradient when PLB is uncoupled from the pump. The increase in catalytic efficiency under gradient-forming conditions suggests that activation of SERCA2a leading to accelerated E2P turnover may be coupled to a decrease in the luminal Ca^{2+} binding affinity. Enhanced E2P turnover can, in principle, increase V_{max} by competing with intravesicular Ca^{2+} binding at the luminal (low-affinity) transport sites on E2P:

$$E2P(Ca_2) \leftrightarrow E2P + 2Ca^{2+}_{i} \rightarrow E2 + P_i$$

The rate at which Ca^{2+} rebinds to E2P depends on the intravesicular Ca^{2+} concentration as well as the level of E2P, which is maintained in a steady state by the rate constants controlling its formation and breakdown. Increasing the rate of breakdown of E2P to P_i will reduce the apparent affinity of E2P for Ca^{2+} ($\uparrow K_{0.5}$) by competing with the formation of $E2P(Ca_2)$. A similar effect on the luminal $K_{0.5}$ for Ca^{2+} can be achieved by increasing the rate of release of Ca^{2+} from $E2P(Ca_2)$ separate from a change in its rate of formation from E2P. In SERCA1, Ca^{2+} de-occlusion from the ADP-insensitive phosphoenzyme controls the rate of release of Ca^{2+} to the intravesicular compartment (*11*, *13*), and activation of spontaneous E2P hydrolysis in the cardiac Ca^{2+}-ATPase (Figure 4B and Table 3) may involve a similar phenomenon. A shift in the poise of intravesicular Ca^{2+} binding to the right will lower the affinity of the luminal transport sites for Ca^{2+}, overcoming the back inhibition from the Ca^{2+} transport gradient while improving the catalytic efficiency. If the increase in catalytic efficiency is linked to an increase in the luminal $K_{0.5}$ for Ca^{2+} binding, then the ability to observe the change in V_{max} will depend on the presence of a Ca^{2+} transport gradient *and the extent of SR* Ca^{2+} *loading*. This may be the crucial factor determining the variability of the results in investigations of Ca^{2+} uptake under V_{max} conditions (*2*, *3*). Future studies aimed at characterizing Ca^{2+} accumulation under variable loading conditions are needed to answer this question about the dependence of V_{max} on the Ca^{2+} gradient and to determine whether an increase in the $K_{0.5}$ for luminal Ca^{2+} binding is associated with the relief of phospholamban inhibition.

REFERENCES

1. Tada, M., Kirchberger, M. A., and Katz, A. M. (1975) Phosphorylation of a 22,000-dalton component of the cardiac sarcoplasmic reticulum by adenosine 3′:5′-monophosphate-dependent protein kinase, *J. Biol. Chem. 250*, 2640−2647.
2. Simmerman, H. K., and Jones, L. R. (1998) Phospholamban: Protein Structure, Mechanism of Action, and Role in Cardiac Function, *Physiol. Rev. 78*, 921−947.
3. Antipenko, A. Y., Spielman, A. I., Sassaroli, M., and Kirchberger, M. A. (1997) Comparison of the kinetic effects of phospholamban phosphorylation and anti-phospholamban monoclonal antibody on the calcium pump in purified cardiac sarcoplasmic reticulum membranes, *Biochemistry 36*, 12903−12910.
4. Tada, M., Ohmori, F., Yamada, M., and Abe, H. (1979) Mechanism of the stimulation of Ca^{2+}-dependent ATPase of cardiac sarcoplasmic reticulum by adenosine 3′:5′-monophosphate-dependent protein kinase. Role of the 22,000-dalton protein, *J. Biol. Chem. 254*, 319−326.
5. Kranias, E. G., Mandel, F., Wang, T., and Schwartz, A. (1980) Mechanism of the stimulation of calcium ion dependent adenosine triphosphatase of cardiac sarcoplasmic reticulum by adenosine 3′,5′-monophosphate dependent protein kinase, *Biochemistry 19*, 5434−5439.
6. Frank, K., Tilgmann, C., Shannon, T. R., Bers, D. M., and Kranias, E. G. (2000) Regulatory role of phospholamban in the efficiency of cardiac sarcoplasmic reticulum Ca^{2+} transport, *Biochemistry 39*, 14176−14182.
7. Shannon, T. R., Chu, G., Kranias, E. G., and Bers, D. M. (2001) Phospholamban decreases the energetic efficiency of the sarcoplasmic reticulum Ca^{2+} pump, *J. Biol. Chem. 276*, 7195−7201.
8. Negash, S., Chen, L. T., Bigelow, D. J., and Squier, T. C. (1996) Phosphorylation of phospholamban by cAMP-dependent protein kinase enhances interactions between Ca^{2+}-ATPase polypeptide chains in cardiac sarcoplasmic reticulum membranes, *Biochemistry 35*, 11247−11259.
9. Froehlich, J. P., and Taylor, E. W. (1975) Transient state kinetic studies of sarcoplasmic reticulum adenosine triphosphatase, *J. Biol. Chem. 250*, 2013−2021.
10. Sumida, M., Wang, T., Schwartz, A., Younkin, C., and Froehlich, J. P. (1980) The Ca^{2+}-ATPase partial reactions in cardiac and skeletal sarcoplasmic reticulum. A comparison of transient state kinetic data, *J. Biol. Chem. 255*, 1497−1503.
11. Mahaney, J. E., Thomas, D. D., and Froehlich, J. P. (2004) The time-dependent distribution of phosphorylated intermediates in the sarcoplasmic reticulum Ca^{2+}-ATPase of skeletal muscle (SERCA1) is not compatible with a linear kinetic model, *Biochemistry 43*, 4400−4416.
12. Toyoshima, C., Nakasako, M., Nomura, H., and Ogawa, H. (2000) Crystal structure of the calcium pump of sarcoplasmic reticulum at 2.6 Å resolution, *Nature 405*, 647−655.
13. Froehlich, J. P., and Heller, P. F. (1985) Transient-state kinetics of the ADP-insensitive phosphoenzyme in sarcoplasmic reticulum: Implications for transient state calcium translocation, *Biochemistry 24*, 126−136.
14. Froehlich, J. P., Taniguchi, K., Fendler, K., Mahaney, J. E., Thomas, D. D., and Albers, R. W. (1997) Complex kinetic behavior in the Na,K- and Ca-ATPases: Evidence for subunit-subunit interactions and energy conservation during catalysis, *Ann. N.Y. Acad. Sci. 834*, 280−296.
15. Andersen, J. P., Lassen, K., and Møller, J. V. (1985) Changes in Ca^{2+} affinity related to conformational transitions in the phosphorylated state of soluble monomeric Ca^{2+}-ATPase from sarcoplasmic reticulum, *J. Biol. Chem. 260*, 371−380.
16. Froehlich, J. P., and Taylor, E. W. (1976) Transient state kinetic effects of calcium ion on sarcoplasmic reticulum adenosine triphosphatase, *J. Biol. Chem. 251*, 2307−2315.
17. Mahaney, J. E., Froehlich, J. P., and Thomas, D. D. (1995) Conformational transitions of the sarcoplasmic reticulum Ca-ATPase studied by time-resolved EPR and quenched-flow kinetics, *Biochemistry 34*, 4864−4879.
18. Ikemoto, N., and Nelson, R. W. (1984) Oligomeric regulation of the later reactions of the sarcoplasmic reticulum calcium ATPase, *J. Biol. Chem. 259*, 11790−11797.

19. Waggoner, J. R., Huffman, J., Griffith, B. N., Jones, L. R., and Mahaney, J. E. (2004) Improved expression and characterization of Ca^{2+}-ATPase and phospholamban in High Five cells, *Protein Expression Purif. 34*, 56−67.
20. Vanderkooi, J. M., Ierokomas, A., Nakamura, N., and Martonosi, A. (1977) Fluorescence energy transfer between Ca^{2+} transport ATPase molecules in artificial membranes, *Biochemistry 16*, 1262−1267.
21. Papp, S., Pikula, S., and Martonosi, A. (1987) Fluorescence energy transfer as an indicator of Ca^{2+}-ATPase interactions in sarcoplasmic reticulum, *Biophys. J. 51*, 205−220.
22. Bigelow, D. J., Squier, T. C., and Inesi, G. (1992) Phosphorylation-dependent changes in the spatial relationship between Ca-ATPase polypeptide chains in sarcoplasmic reticulum membranes, *J. Biol. Chem. 267*, 6952−6962.
23. Vanderkooi, J. M., Papp, S., Pikula, S., and Martonosi, A. (1988) Tryptophan phosphorescence of the Ca^{2+}-ATPase of sarcoplasmic reticulum, *Biochim. Biophys. Acta 957*, 230−236.
24. Birmachu, W., and Thomas, D. D. (1990) Rotational dynamics of the Ca-ATPase in sarcoplasmic reticulum studied by time-resolved phosphorescence anisotropy, *Biochemistry 29*, 3904−3914.
25. Napier, R. M., East, J. M., and Lee, A. G. (1987) State of aggregation of the (Ca^{2+} + Mg^{2+})-ATPase studied by using saturation-transfer electron spin resonance, *Biochim. Biophys. Acta 903*, 365−373.
26. Squier, T. C., Hughes, S. E., and Thomas, D. D. (1988) Rotational dynamics and protein−protein interactions in the Ca-ATPase mechanism, *J. Biol. Chem. 263*, 9162−9170.
27. Sumida, M., Wang, T., Mandel, F., Froehlich, J. P., and Schwartz, A. (1978) Transient kinetics of Ca^{2+} transport of sarcoplasmic reticulum. A comparison of cardiac and skeletal muscle, *J. Biol. Chem. 253*, 8772−8777.
28. Mahaney, J. E., Autry, J. M., and Jones, L. R. (2000) Kinetic studies of the cardiac Ca-ATPase esxpressed in Sf21 cells: New insights on Ca-ATPase regulation by phospholamban, *Biophys. J. 78*, 1306−1323.
29. Froehlich, J. P., Sullivan, J. V., and Berger, R. L. (1976) A chemical quenching apparatus for studying rapid reactions, *Anal. Biochem. 73*, 331−341.
30. Gutfreund, H. (1972) in *Enzymes: Physical Principles*, pp 160−162, John Wiley & Sons, New York.
31. Läuger, P., and Stark, G. (1970) Kinetics of carrier-mediated ion transport across lipid bilayer membranes, *Biochim. Biophys. Acta 211*, 458−466.
32. Dean, W., and Tanford, C. (1978) Properties of a de-lipidated, detergent-activated Ca^{2+}-ATPase, *Biochemistry 17*, 1683−1690.
33. Froehlich, J. P., Bamberg, E., Kane, D. J., Mahaney, J. E., and Albers, R. W. (2000) Contribution of quaternary protein interactions to the mechanism of energy transduction in Na^+/K^+-ATPase, in *Na/K-ATPase and Related ATPases* (Taniguchi, K., and Kaya, S., Eds.) pp 349−356, Elsevier, Amsterdam.
34. Li, J., Xiong, Y., Bigelow, D. J., and Squier, T. C. (2004) Phospholamban binds in a compact and ordered conformation to the Ca-ATPase, *Biochemistry 43*, 455−463.
35. Li, J., Bigelow, D. J., and Squier, T. C. (2004) Conformational changes within the cytoplasmic portion of phospholamban upon release of Ca-ATPase inhibition, *Biochemistry 43*, 3870−3879.
36. Mahaney, J. E., Albers, R. W., Kutchai, H., and Froehlich, J. P. (2003) Phospholamban inhibits Ca^{2+} pump oligomerization and intersubunit free energy exchange leading to activation of cardiac muscle SERCA2a, *Ann. N.Y. Acad. Sci. 986*, 1−3.
37. Toyoshima, C., and Nomura, H. (2002) Structural changes in the calcium pump accompanying the dissociation of calcium, *Nature 418*, 605−611.
38. Mueller, B., Karim, C. B., Negrashov, I. V., Kutchai, H., and Thomas, D. D. (2004) Direct detection of phospholamban and sarcoplasmic reticulum Ca-ATPase interaction in membranes using fluorescence resonance energy transfer, *Biochemistry 43*, 8754−8765.
39. James, P., Inui, M., Tada, M., Chiesi, M., and Carafoli, E. (1989) Nature and site of phospholamban regulation of the Ca^{2+} pump of sarcoplasmic reticulum, *Nature 342*, 90−92.
40. Jones, L. R., Cornea, R. L., and Chen, Z. (2002) Close proximity between residue 30 of phospholamban and cysteine 318 of the cardiac Ca^{2+} pump revealed by intermolecular thiol cross-linking, *J. Biol. Chem. 277*, 28319−28329.
41. Chen, Z., Stokes, D. L., Rice, W. J., and Jones, L. R. (2003) Spatial and dynamic interactions between phospholamban and the canine cardiac Ca^{2+} pump revealed with use of heterobifunctional cross-linking agents, *J. Biol. Chem. 278*, 48348−48356.
42. Chen, Z., Stokes, D. L., and Jones, L. R. (2005) Role of leucine 31 of phospholamban in structural and functional interactions with the Ca^{2+} pump of cardiac sarcoplasmic reticulum, *J. Biol. Chem. 280*, 10530−10539.
43. Toyofuko, T., Kurzydlowski, K., Tada, M., and MacLennan, D. H. (1994) Amino acids Lys-Asp-Asp-Lys-Pro-Val^{402} in the Ca^{2+}-ATPase of cardiac sarcoplasmic reticulum are critical for functional association with phospholamban, *J. Biol. Chem. 269*, 22929−22932.
44. Møller, J. V., Guillaume, L., Marchand, C., Montigny, C., le Maire, M., Toyoshima, C., Staehr Juul, B., and Champeil, P. (2002) Calcium transport by sarcoplasmic reticulum Ca^{2+}-ATPase. Role of the A domain and its C-terminal link with the transmembrane region, *J. Biol. Chem. 277*, 38647−38659.
45. Ikemoto, N., Garcia, A. M., Kurobe, Y., and Scott, T. L. (1981) Non-equivalent subunits in the calcium pump of sarcoplasmic reticulum, *J. Biol. Chem. 256*, 8593−8601.
46. Cantilina, T., Sagara, Y., Inesi, G., and Jones, L. R. (1993) Comparative studies of cardiac and skeletal sarcoplasmic reticulum ATPases. Effect of a phospholamban antibody on enzyme activation by Ca^{2+}, *J. Biol. Chem. 268*, 17018−17025.
47. Inesi, G., Kurzmack, M., Coan, C., and Lewis, D. E. (1980) Cooperative calcium binding and ATPase activation in sarcoplasmic reticulum vesicles, *J. Biol. Chem. 255*, 3025−3031.
48. Knott, G. D. (1979) Mlab: A mathematical modeling tool, *Comput. Programs Biomed. 10*, 271−280.

BI048011I